Self-organization in anisotropic granular materials

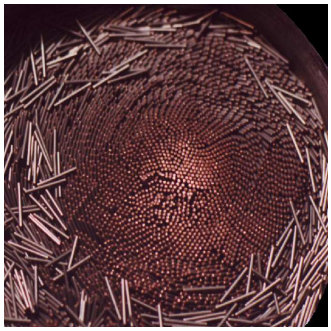

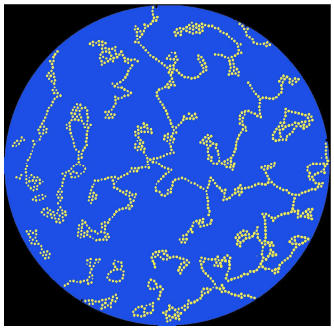

Arshad Kudrolli
Department of Physics, Clark University, Worcester, MA

Collaborators: S. Dorbolo, D. Blair, T. Neicu,
D. Volfson, L. Tsimring (*UCSD*)

Funding: NSF, DOE, Sloan Foundation

Overview

- Impact of shape on dynamics
  - Vortices, ratchets, and bouncing dimers
  - Robo-bug
- Magnetized grains
  - Self-assembly of chains, rings and droplets
- Pictures of other ongoing experiments

Importance of geometry in thermal systems

Entropy maximization leads to long range order Onsager (1949)

Tobacco mosaic virus (X 35,000)
The American Phytopathological Society

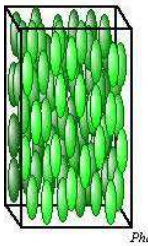

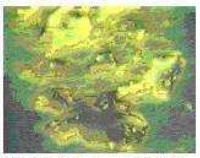

A schematic representation of the nematic phase (left) and a photo of a nematic liquid crystal (above).

Photo courtesy Dr. Mary Neubert LCI-KSU

Photo courtesy of Dr. Mary Neubert LCI-KSU

Packing and avalanching of non-spherical particles

- Random packing for oblate particles can be greater than that for spherical particles (~0.7)
- Prolate grains (rice) shows more irregular avalanche dynamics
- Local angle of repose can be as high as 90 degrees.

Donev *et al*, Science (2004)

Frette *et al*, Nature (1996)

Smectic-like phases of rods in vibrated tall cylinders

- Villarruel, Lauderdale, Mueth, & Jaeger (PRE, 1999) performed experiments with rods inside tall thin cylinders
- Upon vertical vibration, particles are observed to order into smectic like phases
- Ordering starts at the boundaries and propagates inward

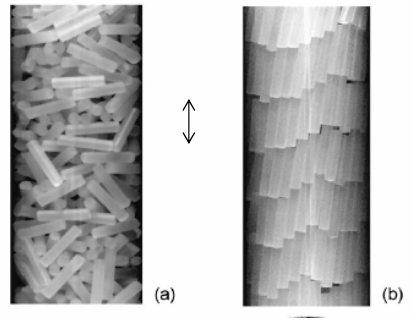

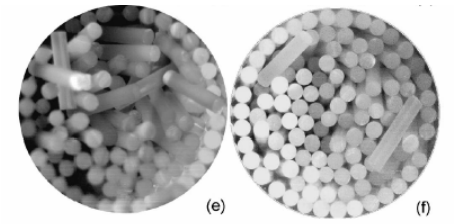

Experimental setup

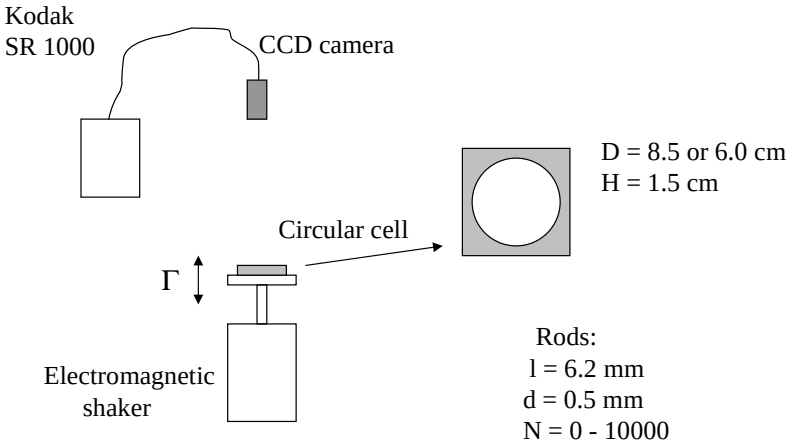

Rods:
l = 6.2 mm
d = 0.5 mm
N = 0 - 10000

(Thanks to S. Fraden)

$a(t) = \Gamma \sin(2 \pi f t)$

f = 20 - 100 Hz

Self-organized vortex patterns observed

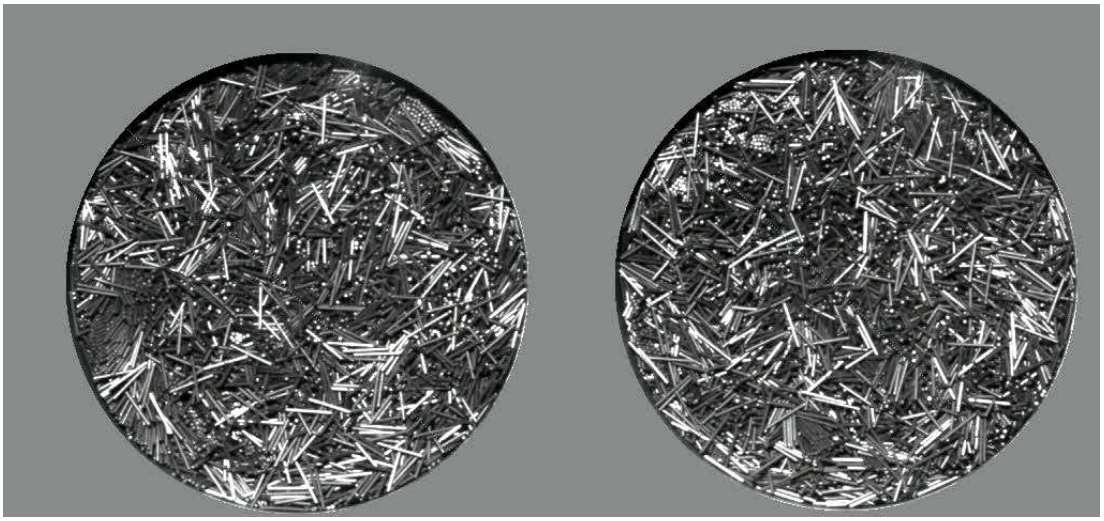

$\Gamma = 3.4$ $\Gamma = 4.2$

f = 50 Hz, N = 8000

Image of the inclined rods

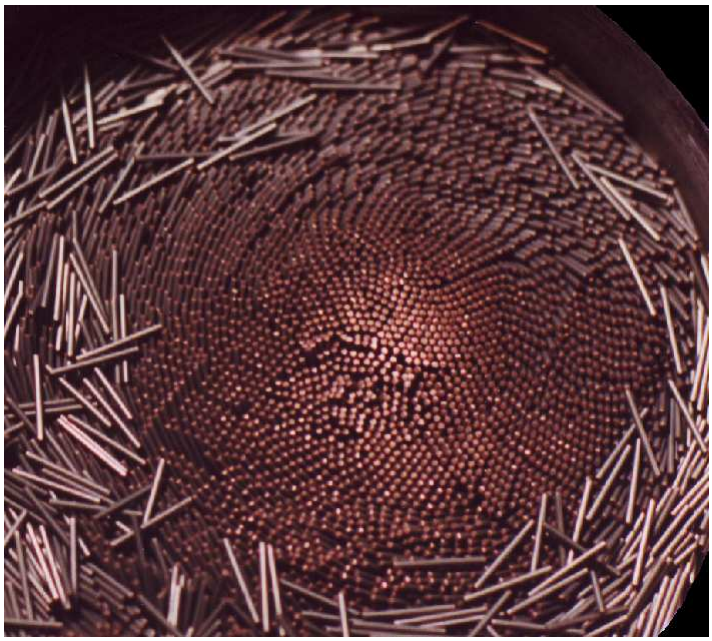

Angle of inclination of the rods

$\theta = \sin^{-1}(d / x)$

$n_\phi = 0.42$

Phase Diagram

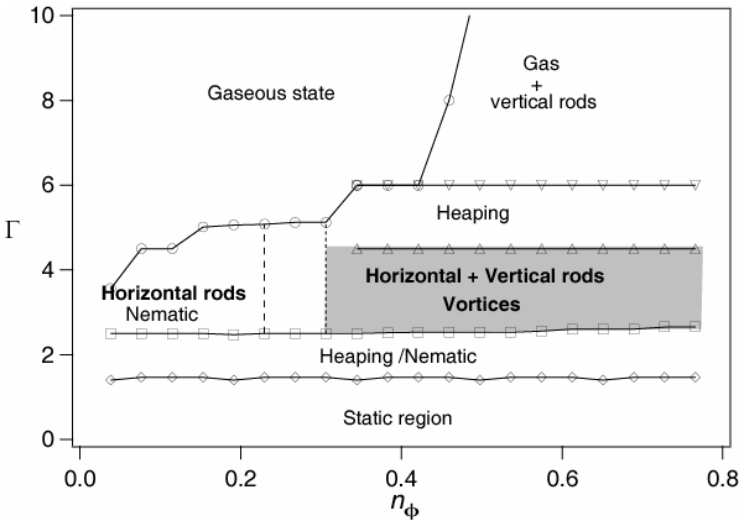

$\Gamma = A (2 \pi f)^2 / g$ $\quad\quad$ $n_\phi = N / N_{max}$

N = Number of rods

N_{max} = Rods required to obtain a vertically aligned monolayer

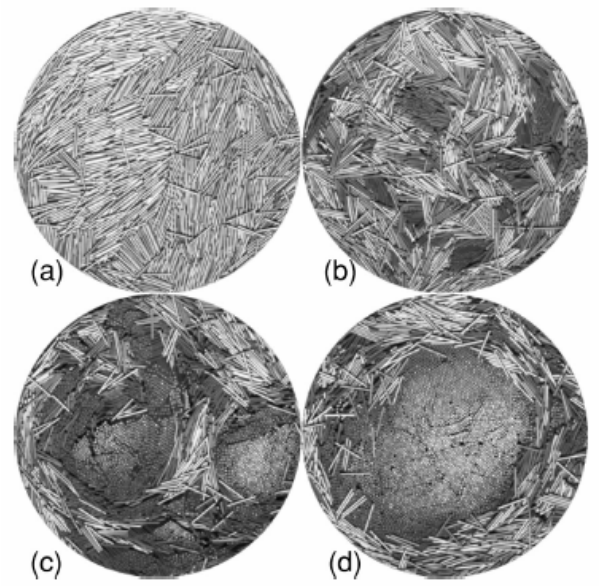

$n_\phi = 0.152$ $\quad$ $n_\phi = 0.344$

$n_\phi = 0.551$ $\quad$ $n_\phi = 0.535$

Vortex

Are the rods vertical because the vibrations are vertical?

Horizontal shaking

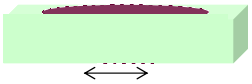

$\Gamma = 1.04$, $n_\phi = 0.61$, f = 30 Hz

- Domains with vertical rods observed
- Vortices are not observed

Why are rods vertically aligned?

Void filling mechanism

• A vertically aligned rod can fall in to a smaller void then a horizontal one.

n_v P.E. > n_h P.E.

• A vertically aligned rod in the center of a vertical pack cannot easily hop out and become horizontal.

Growth of the vertical domains

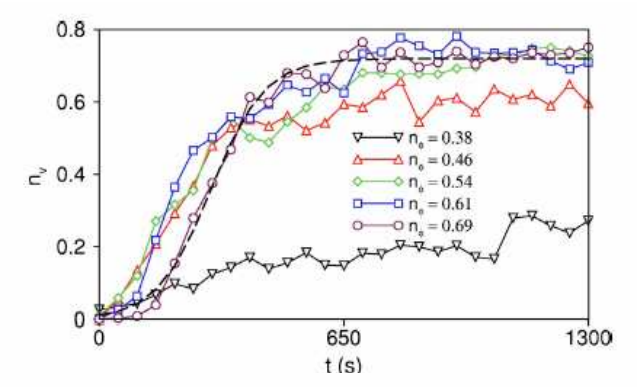

$$\frac{\partial n_v}{\partial t} = \alpha n_v(\beta - n_v),$$

Phenomenological Model of Coarsening and Vortex formation developed by Aranson and Tsimring (2003)

Velocity Field

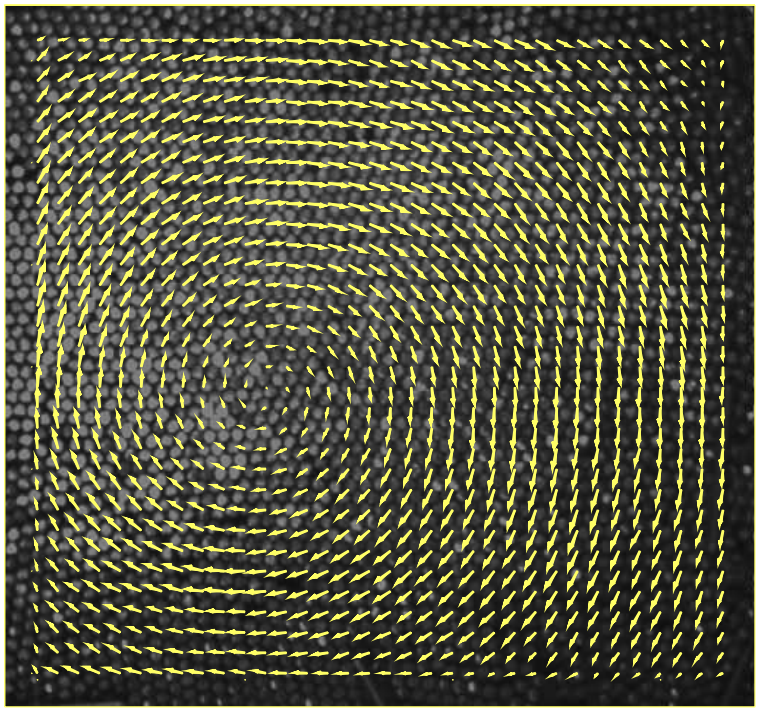

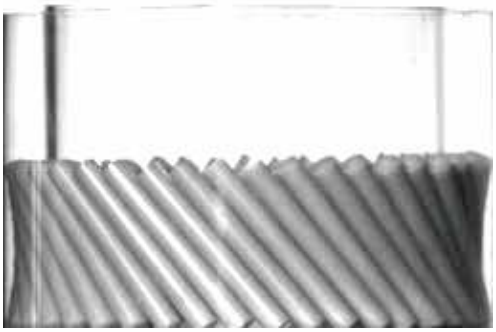

2.5 g, 60 Hz

Teflon rods of length 5.1 cm and diameter 0.6 cm are vibrated inside a 1D annulus

Experimental Data

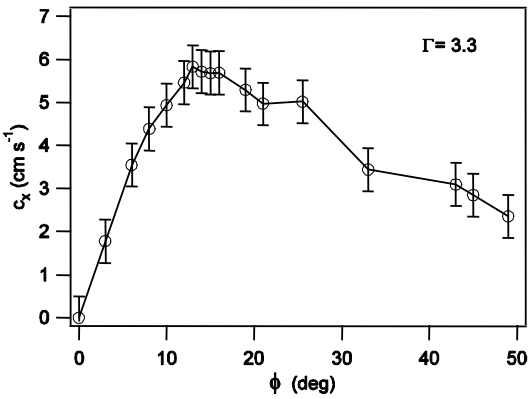

Velocity vs. tilt

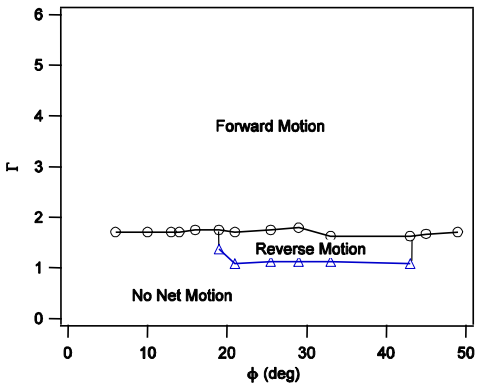

Phase diagram

Molecular dynamics simulations

Dimitri Volson and Lev Tsimring, UCSD

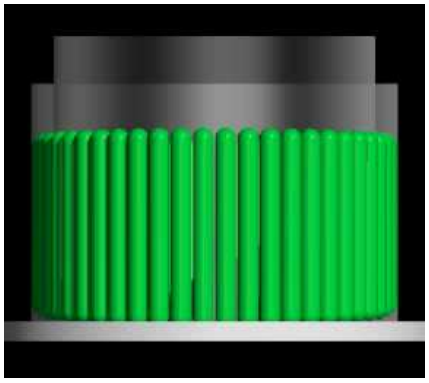

Rod parameters match with experiments

Motion ceases when friction between rods and the bottom of container is decreased to zero

Simulations

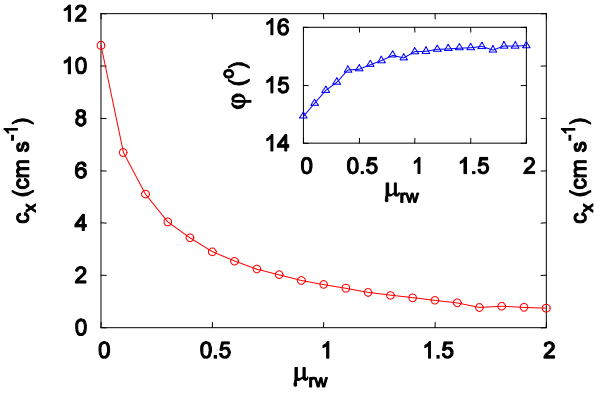

Velocity versus rod-side wall friction

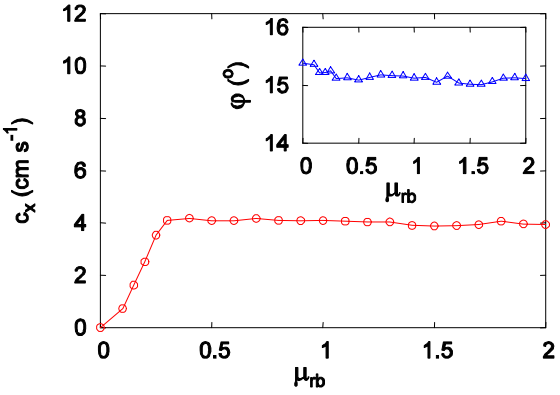

Velocity versus rod-bottom friction

Collision of a rod and the plate

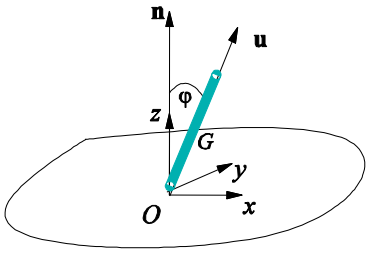

$$m\, dc = dP$$
$$I\, d\omega = -\, l/2\, u \times dP$$

Apply Newton's law at contact point to relate velocity before and after collision

During collision, three possible scenarios:

- slip
- slip-stick
- slip reversal

Velocity as a function of tilt and driving veloicty

$$c_x = f(\varepsilon, \mu, \phi)\, V_0$$

To close the equation we assume:

(i) $\omega = 0$ before collision of the rod with plate

(ii) horizontal velocity before and after collision is the same

(iii) vertical velocity simply changes sign

- D. Volson, A.K., L. Tsimring, PRE (2004)

Comparison of model with simulations and experiments

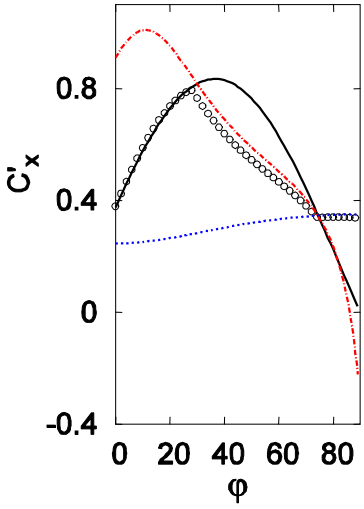

Model / 2D simulation

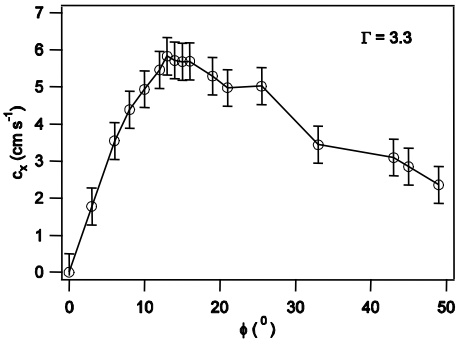

Experiment

Motion of an anisotropic particle on a vibrated plate

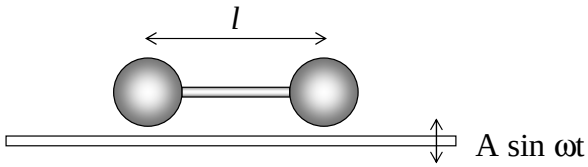

- Complex modes observed depending on the relative phase of motion of the two particles on the plate

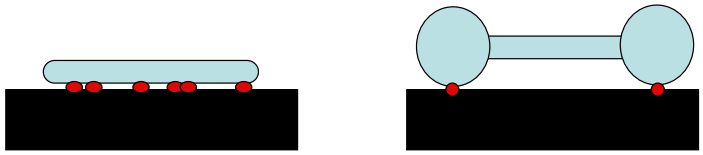

Rod/Dimer

Dynamics of a bouncing dimer

Flutter mode

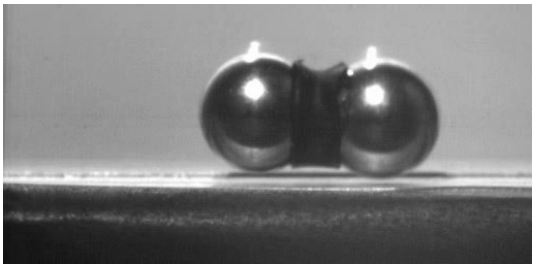

Jump mode

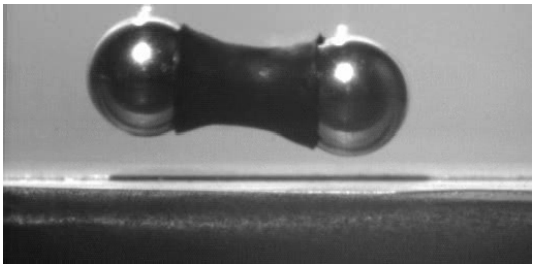

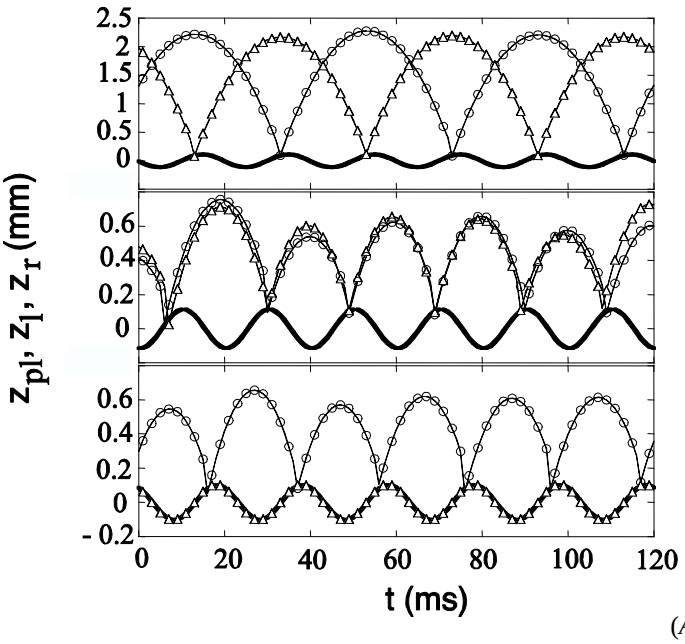

Flutter mode

Jump mode

Drift mode

(A_r = 3.8, f = 50 Hz, Γ = 0.9)

Drift Mode

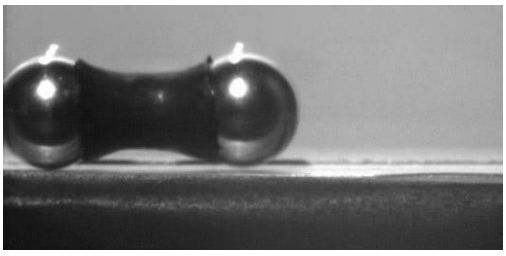

1D

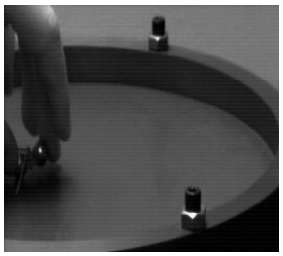

2D

Plate surface is smooth and therefore our situation is different from previous examples of ratchets

e.g. Derenyi *et al*, Chaos (1998)

Collision of the dimer with the plate

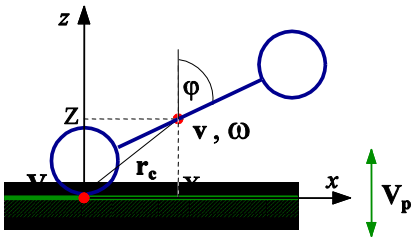

Newton's laws:

$$m\,\dot{\mathbf{v}} = \sum_c \mathbf{F}^c + m\mathbf{g}, \qquad I\,\dot{\omega} = \sum_c \mathbf{r}_c \times \mathbf{F}^c \tag{1}$$

m: mass *I*: moment of inertia

Force at contact points: $F^c = (F_x^c, 0, F_z^c)$ During slip: $F_x^c = -\mathrm{sgn}\,U_c \mu F_z^c$

Stick-slip: $|F_x^c| = \mu_s F_z^c$ μ_s depends on the contact time

Single collision
1: Continuous slide
2: Slip-stick
3: Slip reversal

Double collision
1: Double slide
2: Double slip-stick
3. Double slip reversal

1: Rolling without slip
2: Rolling with slip

Need to consider all possible collisions to obtain correct dynamics

SINGLE COLLISIONS

In this section we write down the formulas for an isolated collision between a dimer and a plate. These formulas are deduced from our previous paper (with some change of the notations) [2]. The general mappings which relate CM velocities immediately after collision to the CM velocities right before collision may be written as,

$$u^a = F_u(u^b, v^b, \omega^b, \phi) \tag{2}$$
$$v^a = F_v(u^b, v^b, \omega^b, \phi) \tag{3}$$
$$\omega^a = F_\omega(u^b, v^b, \omega^b, \phi) \tag{4}$$

A. Slide

The continuous sliding condition reads

$$j\left[u^b - \omega^b Z + \frac{XZ + j\hat{\mu}(K^2+Z^2)}{K^2+X^2+j\hat{\mu}XZ}(v^b + \omega^b X - V_{pl})(1+\epsilon)\right] > 0 \tag{5}$$

Here $j = \mathrm{sgn}(u^b - \omega^b Z)$ is the direction of the horizontal projection of the contact point velocity in the beginning of the contact, and the expression in square brackets is the horizontal contact velocity in the end of the contact. If this condition is satisfied, the colliding ball slides throughout the collision without changing direction. The mapping for the CM velocities at the end of the collision reads:

$$F_u(u,v,\omega,\phi) = u + \frac{j\hat{\mu}(1+\epsilon)K^2(v - V_{pl} + \omega X)}{K^2+X^2+j\hat{\mu}XZ}, \tag{6}$$
$$F_v(u,v,\omega,\phi) = v - \frac{(v - V_{pl} + \omega X)(1+\epsilon)K^2}{K^2+X^2+j\hat{\mu}XZ} \tag{7}$$
$$F_\omega(u,v,\omega,\phi) = \omega - \frac{(v - V_{pl} + \omega X)(1+\epsilon)(X + j\hat{\mu}Z)}{K^2+X^2+j\hat{\mu}XZ} \tag{8}$$

Event driven simulation based on single and double collision rules

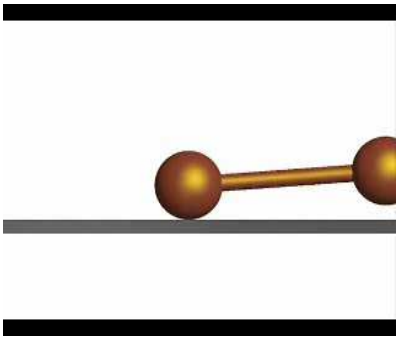

$\Gamma = 0.9$, $f = 25$ Hz, $A_r = 3.8$

The friction coefficients and inelasticity parameters used were directly measured from the experiment

Velocity versus aspect ratio

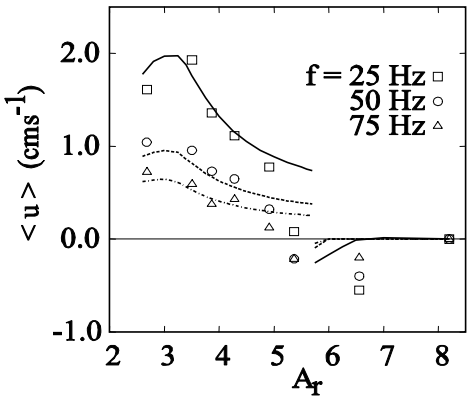

Criterion for reverse motion

$$\hat{\mu}_s (A^2 + 7/5) > A$$

The average velocity measured in experiments is similar to those obtained in the simulations

Dimer can drift in the forward (in the direction of bouncing end), or backward direction depending on the aspect ratio A_r

A dimer can climb an oscillating hill

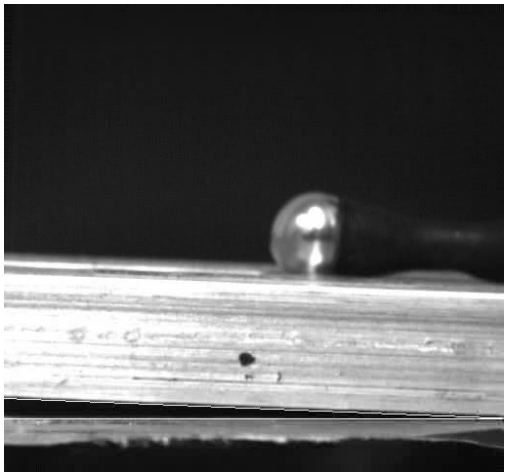

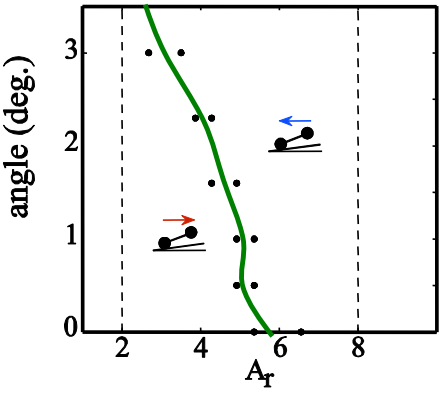

$\theta = 3$ deg, $f = 50$ Hz, $\Gamma = 0.9$

S. Dorbolo, D. Volfson, L. Tsimring, A.K., preprint

Asymmetric Dimer Ratchets: Robo-Bug

"Simplest" examples of noise driven motors

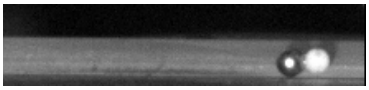

Steel-Glass beads

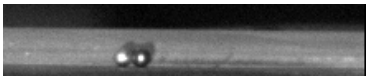

Aluminum-Steel beads

- Symmetry breaking leads to translation motion in rods and dimers

Magnetized Granular Matter

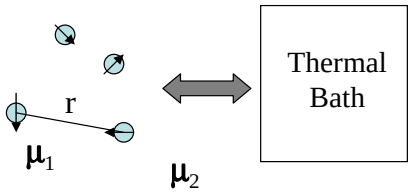

Dipole interaction:

$$U(r) = (\boldsymbol{\mu}_1 . \boldsymbol{\mu}_2) / r^3 - 3 (\boldsymbol{\mu}_1 . \mathbf{r}) (\boldsymbol{\mu}_2 . \mathbf{r}) / r^5$$

Granular matter with "long" range interaction
Also representative of polar fluids – e.g. Ferrofluids

Dipoles like to line up thus creating chains, this anisotropic nature lead to novel phases

Simulations are difficult, and the issue is complicated theoretically

Dipolar hard sphere model (DHSM) (No dissipation)

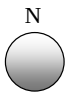

$$U(r) = U_{hs} + (\boldsymbol{\mu}_1 . \boldsymbol{\mu}_2) / r^3 - 3 (\boldsymbol{\mu}_1 . \mathbf{r}) (\boldsymbol{\mu}_2 . \mathbf{r}) / r^5$$

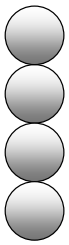

Each dipole alignment lowers P.E. by $U = 2 \mu/d^3$

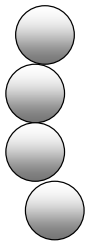

Energy is required to bend, but energy of a ring is in fact lower once number of particles equals four

DSMC on the DHSM find a transition from a gas composed of free particles to a liquid composed of a network of chains (reference point)

Experimental system

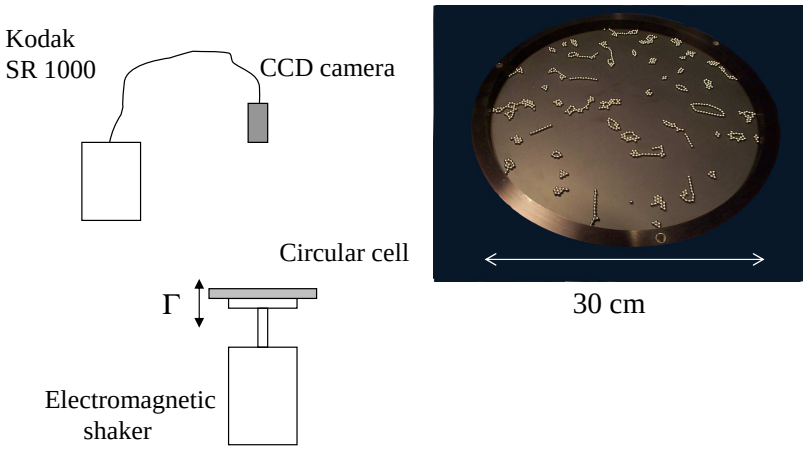

Magnetized beads vibrated inside a container

Examples of Cluster Seeds

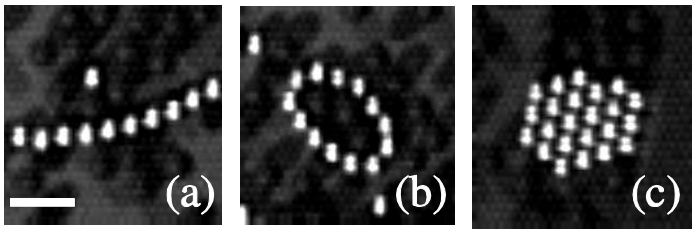

Chains Rings Crystallite

- Because of dipolar field, particles align in chains.
- Rings are energetically more favorable when chain length exceeds four particles

Movies

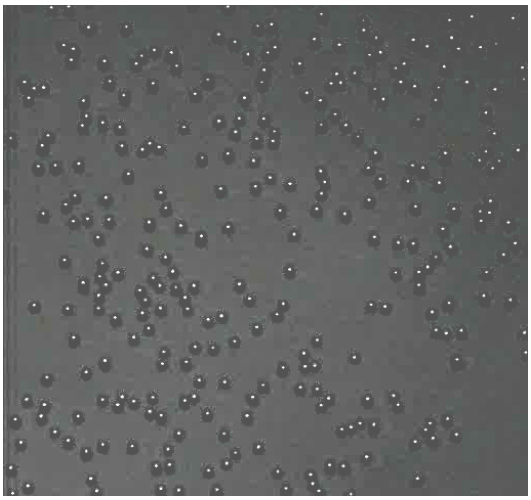

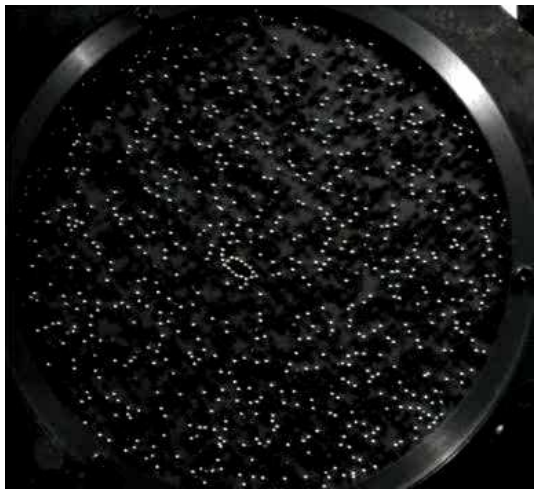

Growth of Clusters

Phases observed as a function of granular temperature and volume fraction of particles

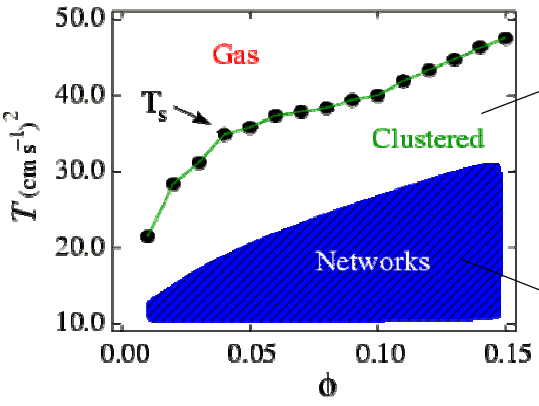

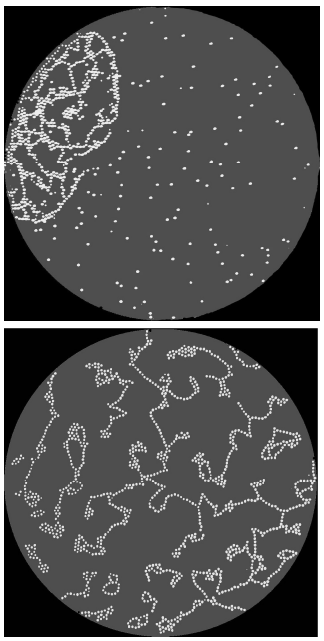

Compact clusters or networks are observed to grow depending on the rate of cooling

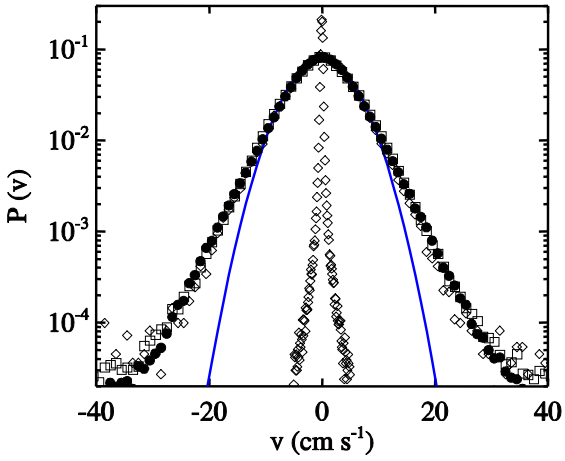

The velocity distribution of particles in the cluster is significantly narrower than that of the magnetic and non-magnetic particles in the surrounding gas phase

The size of the cluster and its granular temperature

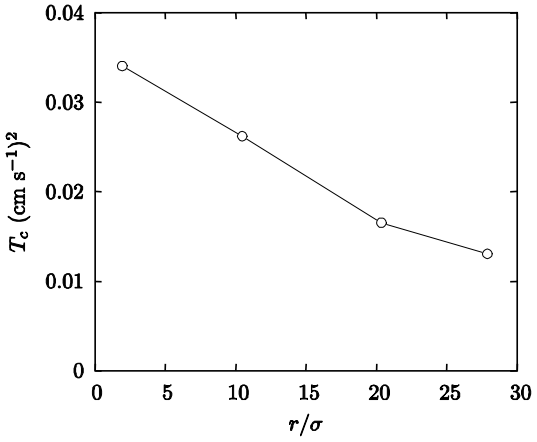

Equipartition is not observed

Growth of the radius of gyration

$T = T_s$

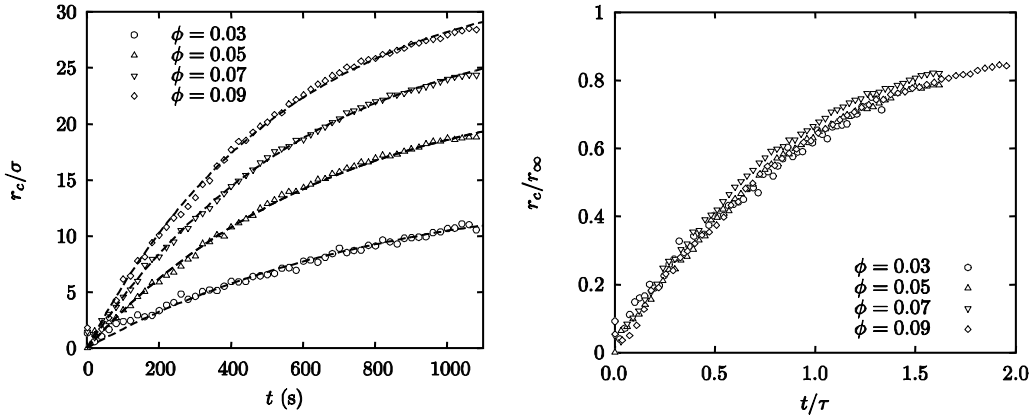

Growth described by $R_c = r_\infty [1 - \exp(- t/\tau)]$

Growth of the radius of gyration

$T < T_s$

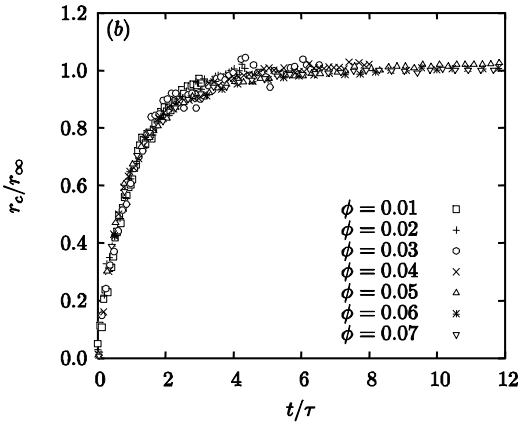

Growth also described by $R_c = r_\infty (1 - \exp(- t/\tau))$

Compactness of Cluster

$T < T_s$

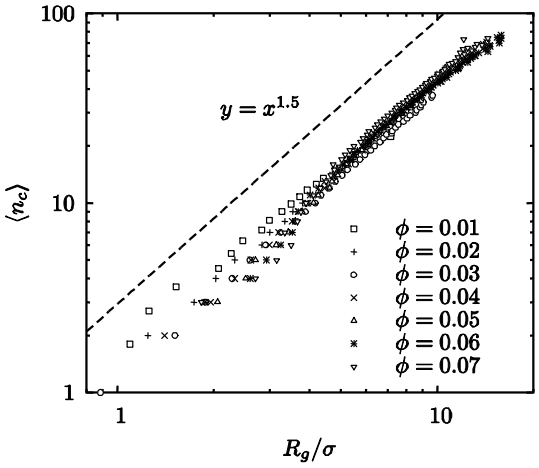

Growth also described by $n_c = \alpha R_g^d$

Migration of Cluster

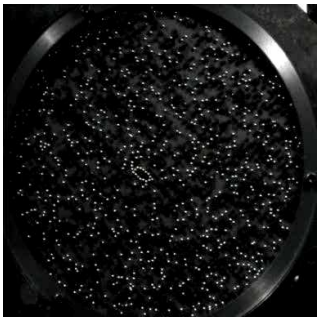

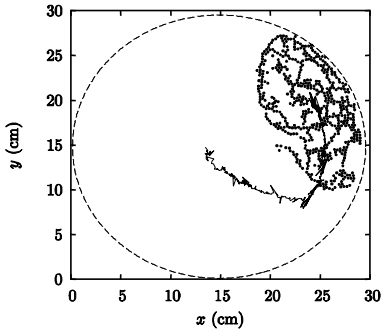

Pressure due to gas particles colliding with cluster keeps the cluster pinned to the side wall.
Similar effects observed in bidisperse colloids - Depletion Force

Summary

- Granular matter with dipolar cohesive interaction
  - Compact structures observed
  - Chains and rings are observed to be unstable in the experiments
- Clustering transition observed below a critical temperature which depends on volume fraction of particles
- The temperature of the particles in the clusters is significantly lower than that of the surrounding gas phase

See: PRE (2004) &

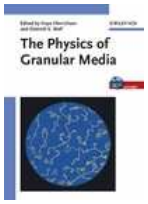

Complex Matter and Biodynamics Laboratory, Clark University

http://physics.clarku.edu/~akudrolli

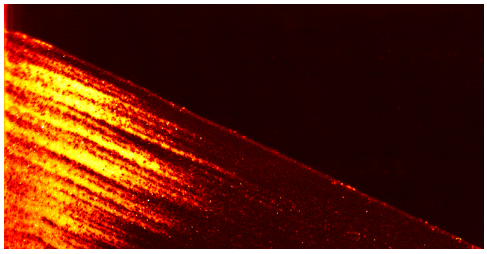

Wet Granular Matter

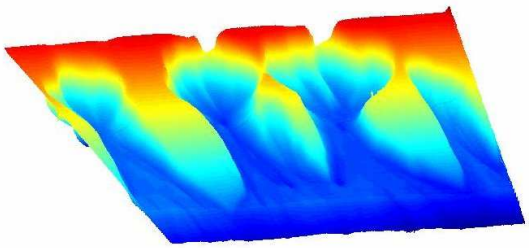

Erosion Patterns

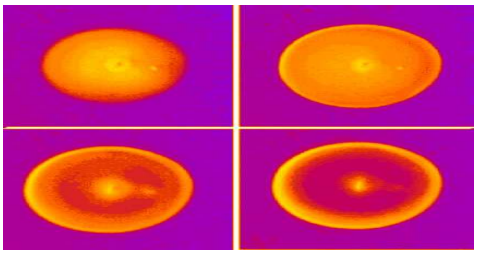

Bacterial Trek

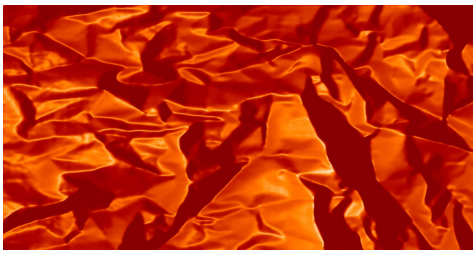

Crumpling

(Samadani, Xu, Smith, Lobkovsky, Rothman, Delprato, Tsimring, Blair)

June talk: Slow dense granular flows

- More typical, e.g. silo drainage
- Particles almost always in contact, geometry dominated flow

Of interest: velocity fields, residence time, particle diffusion

Applications: Hourglass, Nuclear pebble bed reactors

- Granular flows are advective and considerably less diffusion is observed then predicted by models
- Imaging 3D flow using index-matching

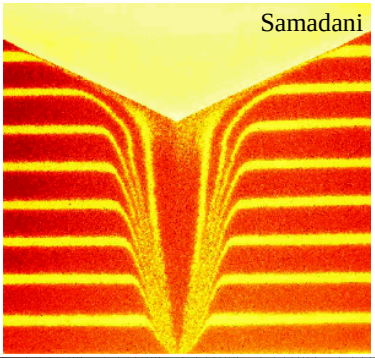

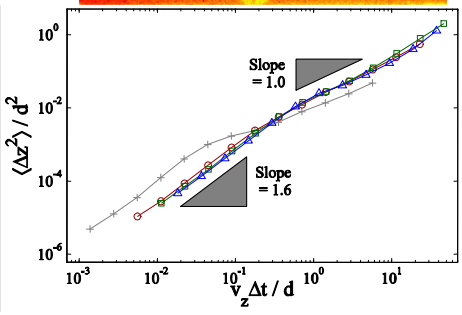

Choi *et al*, PRL (2004)